Magnitudes and Relative Orientations of Chemical Shielding, Dipolar and *J* Coupling Tensors for Isolated $^{31}P-^{31}P$ Spin Pairs Determined by Iterative Fitting of ^{31}P MAS NMR Spectra

Stephan Dusold,[†] Elke Klaus,[†] Angelika Sebald,*[,†] Mads Bak,[‡] and Niels Chr. Nielsen*[,‡]

Contribution from the Bayerisches Geoinstitut, Universität Bayreuth, D-95440 Bayreuth, Germany, and Department of Chemistry, University of Aarhus, DK-8000 Aarhus C, Denmark

Received March 20, 1997. Revised Manuscript Received May 14, 1997[⊗]

Abstract: Accurate measurements of the magnitudes and relative orientations of chemical shielding, *J* coupling and dipolar coupling tensors for isolated homonuclear $^{31}P-^{31}P$ spin pairs, using standard ^{31}P MAS NMR experiments in conjunction with efficient numerical simulation and iterative fitting procedures are described. For a series of transition-metal phosphine complexes $(R_3P)_2MX_2$, containing pairs of crystallographically equivalent phosphorus atoms such that they constitute isolated magnetically nonequivalent $^{31}P-^{31}P$ spin-pair systems, it is demonstrated that the combined effects from MAS averaging, $n = 0$ rotational resonance dipolar recoupling, and *J* recoupling lead to ^{31}P MAS NMR spectra with detailed structural features. These features are highly dependent on the tensorial interactions as well as on the applied external magnetic field strength and MAS frequency. The experimental observations are reproduced by numerically exact computer simulations. Iterative fitting of ^{31}P MAS spectra, recorded under various experimental conditions, allows for determination of accurate parameters for the isotropic and anisotropic interactions characterizing the $^{31}P-^{31}P$ spin pair. In particular, we demonstrate that the orientation of the chemical shielding tensors relative to each other and relative to the internuclear axis can be determined with high accuracy.

Introduction

The past years have witnessed a considerable interest in using ^{31}P solid-state NMR spectroscopy for the retrieval of information about structure and dynamics for a large variety of phosphorus-containing organic and inorganic solids. For solids containing spatially well isolated phosphorus atoms, standard powder NMR methods suffice to extract information about magnitudes of the respective ^{31}P chemical shielding tensors. For solids containing two (or more) ^{31}P spins coupled either indirectly by *J* coupling or through space by dipolar coupling, solid-state NMR may under favorable conditions provide additional detailed information about internuclear distances, coupling networks, and relative orientations of anisotropic interaction tensors. This holds true, in particular, for isolated $^{31}P-^{31}P$ spin pairs where it has been shown that useful information about internuclear distances and relative orientations of ^{31}P chemical shielding tensors may be extracted from powder[1,2] or single-crystal[3] ^{31}P NMR spectra. For larger spin systems the spectra often become exceedingly complex and difficult to interpret in terms of parameters of the various isotropic and anisotropic interactions.

Among the isolated $^{31}P-^{31}P$ spin pairs, those composed of chemically equivalent but magnetically inequivalent ^{31}P spins have attracted particular interest. From a structural point of view such spin pairs are of interest because the nuclei and their local environment are interrelated by rotation-reflection symmetry operations within the molecular symmetry group. From a NMR point of view such spin pairs are particularly interesting because the two spins in this case exhibit identical isotropic chemical shifts which effectively prevents averaging of the nonsecular terms of the dipolar interaction even under magic-angle spinning (MAS) conditions. This recoupling,[1,4,5] often referred to as $n = 0$ rotational resonance, implies that it is possible to obtain detailed information about the anisotropic interactions from MAS spectra which, in addition, provide conditions of fairly high spectral resolution and sensitivity. Especially in the so-called slow spinning regime, the combination of MAS averaging, *J* recoupling, and $n = 0$ rotational resonance leads to complicated spinning side band patterns, the structure of which is highly sensitive to indirect *J* and to dipolar coupling as well as to anisotropic chemical shielding interactions. In particular, it is important that the spectral lineshapes depend on the recoupled dipolar interaction: this dependency enables the determination of the relative orientations of the chemical shielding tensors with respect to the internuclear axis.

In ^{13}C MAS NMR spectroscopy, major efforts have been made to design and optimize dipolar recoupling schemes[5,6] for the exploitation of precisely this useful dependency for purposes of structural analysis also for those conditions where no $n = 0$ rotational resonance exists. In ^{13}C NMR, dipolar recoupling methods are now commonly used, despite the fact that usually specific ^{13}C isotopic labeling is required. The more surprising it seems that for isolated $^{31}P-^{31}P$ spin pairs—where even no extra-effort with isotopic labeling is necessary—little attention has so far been devoted to ^{31}P MAS NMR as a means to extract accurate parameters for the anisotropic interactions of dipolar

* Authors to whom correspondence should be addressed.
[†] Universität Bayreuth.
[‡] University of Aarhus.
[⊗] Abstract published in *Advance ACS Abstracts,* July 1, 1997.
(1) Kubo, A.; McDowell, C. A. *J. Chem. Phys.* **1990**, *92*, 7156.
(2) Nakai, T.; McDowell, C. A. *J. Am. Chem. Soc.* **1994**, *116*, 6383.
(3) Lumsden, M. D.; Wasylishen, R. E.; Britten, J. F. *J. Phys. Chem.* **1995**, *99*, 16602.
(4) Maricq, M. M.; Waugh, J. S. *J. Phys. Chem.* **1979**, *70*, 3300.
(5) (a) Levitt, M. H.; Raleigh, D. P.; Creuzet, F.; Griffin, R. G. *J. Chem. Phys.* **1990**, *92*, 6347. (b) Schmidt, A.; Vega, S. *J. Chem. Phys.* **1992**, *96*, 2655. (c) Nielsen, N. C.; Creuzet, F.; Griffin, R. G.; Levitt, M. H. *J. Chem. Phys.* **1992**, *96*, 5668. (d) Nakai, T.; McDowell, C. A. *J. Chem. Phys.* **1992**, *96*, 3452. (e) Bennett, A. E.; Griffin, R. G.; Vega, S. In *NMR Basic Principles and Progress*; Blümich, B., Ed.; Springer Verlag: Berlin, 1994; Vol. 33, p 1−78.

S0002-7863(97)00890-1 CCC: $14.00

coupled $^{31}P-^{31}P$ spin pairs: spectral lineshape simulations have only been reported for ^{31}P MAS spectra of an isolated *pyro*-phosphate, $P_2O_7^{4-}$ moiety,[1] and very recently for two organophosphorus compounds.[7] In contrast, several studies on $^{31}P-^{31}P$ spin pairs displaying $n = 0$ rotational resonance effects have instead focused on aspects of J recoupling[8−11] or have applied more complicated and time-consuming experimental methods such as two-dimensional spin-echo experiments on static powders[2] to separate effects from the various spin-pair interactions in distinct spectral dimensions. Variable-angle spinning has been used as a method to reduce the effects of the structurally important dipolar interaction while employing the isotropic J coupling to establish information about the relative orientation of chemical shielding tensors.[12] The practical applicability of isotropic J coupling related approaches for the extraction of orientational chemical shielding tensor parameters is constrained to cases fulfilling combined requirements of a limiting maximum spread of the chemical shielding tensors and a limiting minimum in magnitude of the isotropic J coupling.

In this study, we demonstrate that straightforward ^{31}P MAS NMR, in combination with numerically exact simulation and iterative fitting of the experimental spectra, represents an attractive route to detailed and accurate information about magnitudes and relative orientations of dipolar coupling and chemical shielding tensors for isolated $^{31}P-^{31}P$ spin pairs displaying $n = 0$ rotational resonance effects. Exemplified by the analysis of ^{31}P MAS NMR spectra of three different such $^{31}P-^{31}P$ spin-pair systems (obtained at different external magnetic field strengths and MAS frequencies), it is shown that owing to the high sensitivity of the spectral lineshapes in these ^{31}P MAS NMR spectra to the combined effects of external experimental parameters and internal anisotropic NMR interactions, orientational spin-pair parameters may be obtained with high accuracy. Our $^{31}P-^{31}P$ spin pairs are represented by three different transition-metal phosphine complexes where the presence of bulky organic ligands attached to the P atoms ensures that we are dealing with isolated $^{31}P-^{31}P$ spin pairs. The selection of compounds is such that a variety of relative magnitudes of anisotropic interactions is represented by compounds **1**−**3.**

Experimental Section

Compounds **1**,[13] **2**,[14] and **3**[15] were synthesized following published methods. All ^{31}P MAS NMR spectra were obtained using conventional Hartmann−Hahn cross-polarization (CP) with CP contact times of typically 2−3 ms, with recycle delays of ca. 3−5 s (**2** and **3**) and 30 s (**1**), and with $\pi/2$ pulse durations in the range 2.5−4 μs. ^{31}P MAS NMR spectra were recorded on Bruker MSL 100, MSL 200, MSL 300, and DSX 500 NMR spectrometers, corresponding to ^{31}P Larmor frequencies of 40.5, 81.0, 121.5, and 202.5 MHz, respectively. Standard double-bearing probes and ZrO_2 rotors (4 and 7 mm diameter) were used; spinning frequencies were in the range 0.8−12 kHz. The stability of the MAS frequencies was actively controlled within ±1 Hz, using home-built equipment. The 2D ^{31}P spin-echo experiment on a static powder sample of **3** was performed as described in ref 2, except that the plain π pulse has been replaced by a composite π pulse.[16] Simulations of the 2D ^{31}P spin-echo spectrum are based on eqs 5 and 7 given in ref 2. ^{31}P chemical shielding is reported relative to external 85% H_3PO_4, $\sigma_{iso} \equiv 0$; shielding notation ($\sigma = -\delta$ [ppm]) will be used throughout text and Table 1; ppm scales plotted in figures are δ scales. All calculations were performed on a Digital Alpha 1000 4/200 workstation and typically required 4−8 min of CPU time for a calculation including 1024−2048 points, 232 crystallite orientations selected for $0 \le \alpha_{CR} \le 2\pi$ and $0 \le \beta_{CR} \le \pi$ according to the REPULSION method,[17] 20−30 steps $0 \le \gamma_{CR} \le 2\pi$ averaging by time-translation of the Hamiltonian,[5] and integration of the homogeneous evolution in 30−40 steps over the rotor period.

Chart 1

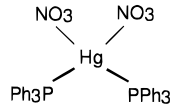

1

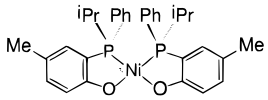

2

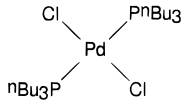

3

Numerical Simulation and Iterative Fitting

The theory describing the evolution of the density matrix for isolated pairs of spin-1/2 nuclei has been described extensively in the literature.[5,6] Therefore, here we restrict ourselves to a very condensed description of the theory and definitions required for numerical simulation and iterative fitting of $^{31}P-^{31}P$ spin-pair systems as described in this work.

In the Zeeman interaction representation, the high-field truncated Hamiltonian of a homonuclear S_A-S_B spin-pair system may conveniently be written

$$H(t) = \omega_A(t)S_{Az} + \omega_B(t)S_{Bz} + \omega_D(t)(3S_{Az}S_{Bz} - S_A\cdot S_B) + \omega_J S_A\cdot S_B \quad (1)$$

with A and B referring to chemical shielding, D to dipolar coupling, and J to indirect coupling (assumed isotropic). For each of these interactions the time and orientation dependence may be expressed in terms of a Fourier series

$$\omega_\lambda(t) = \sum_{m=-2}^{2} \omega_\lambda^{(m)} \exp(im\omega_r t) \quad (2)$$

(6) (a) Gullion, T.; Vega, S. *Chem. Phys. Lett.* **1992**, *194*, 423. (b) Bennett, A. E.; Ok, J. H.; Griffin, R. G.; Vega, S. *J. Chem. Phys.* **1992**, *96*, 8624. (c) Sodickson, D. K.; Levitt, M. H.; Vega, S.; Griffin, R. G. *J. Chem. Phys.* **1993**, *98*, 6742. (d) Tycko, R.; Smith, S. O. *J. Chem. Phys.* **1993**, *98*, 932. (e) Tycko, R. *J. Am. Chem. Soc.* **1994**, *116*, 2217. (f) Nielsen, N. C.; Bildsøe, H.; Jakobsen, H. J.; Levitt, M. H. *J. Chem. Phys.* **1994**, *101*, 1805. (g) Zhu, W.; Klug, C. A.; Schaefer, J. *J. Magn. Reson. A* **1994**, *108*, 121. (h) Baldus, M.; Tomaselli, M.; Meier, B. H.; Ernst, R. R. *Chem. Phys. Lett.* **1994**, *230*, 329. (i) Sun, B.-Q.; Costa, P. R.; Kocisko, D.; Lansbury, P. T.; Griffin, R. G. *J. Chem. Phys.* **1995**, *102*, 702. (j) Geen, H.; Titman, J. J.; Gottwald, J.; Spiess, H. W. *J. Magn. Reson. A* **1995**, *114*, 264. (k) Gottwald, J.; Demco, D. E.; Graf, R.; Spiess, H. W. *Chem. Phys. Lett.* **1995**, *243*, 314. (l) Lee, Y. K.; Kurur, N. D.; Helmle, M.; Johannessen, O. G.; Nielsen, N. C.; Levitt, M. H. *Chem. Phys. Lett.* **1995**, *242*, 304. (m) Gregory, D. M.; Mitchell, D. J.; Stringer, J. A.; Kiihne, S.; Shiels, J. C.; Callahan, J.; Mehta, M. A.; Drobny, G. P. *Chem. Phys. Lett.* **1995**, *246*, 654. (n) Bak, M.; Nielsen, N. C. *J. Chem. Phys.* **1997**, *106*, 7587.

(7) Wu, G.; Sun, B.-Q.; Wasylishen, R. E.; Griffin, R. G. *J. Magn. Reson. A* **1997**, *124*, 366.

(8) Nakai, T.; Challoner, R.; McDowell, C. A. *Chem. Phys. Lett.* **1991**, *180*, 13.

(9) Challoner, R.; Nakai, T.; McDowell, C. A. *J. Chem. Phys.* **1991**, *94*, 7038.

(10) Wu, G.; Wasylishen, R. E. *J. Chem. Phys.* **1993**, *98*, 6138.

(11) Klaus, E.; Sebald, A. *Angew. Chem., Int. Ed. Engl.* **1995**, *34*, 667.

(12) Wu, G.; Wasylishen, R. E. *J. Chem. Phys.* **1994**, *100*, 4828.

(13) Allmann, T.; Lenkinski, R. E. *Inorg. Chem.* **1986**, *25*, 3202.

(14) Heinicke, J.; Klaus, E.; Koesling, M.; Pritzkow, H.; Sebald, A. *Solid State Nucl. Magn. Reson.* Submitted for publication.

(15) (a) Hartley, F. R. *Organomet. Chem. Rev. A* **1970**, *6*, 119. (b) *Transition-Metal Complexes of Phosphorus, Arsenic and Antimony Ligands*; McAuliffe, C. A., Ed.; Macmillan: London, 1973.

(16) Levitt, M. H. *Prog. Nucl. Magn. Reson. Spectrosc.* **1986**, *18*, 61.

(17) Bak, M.; Nielsen, N. C. *J. Magn. Reson. A* **1997**, *125*, 132.

where ω_r denotes the spinning frequency in angular units. The Fourier coefficients take the general form

$$\omega_\lambda^{(m)} = \omega_{\text{iso}}^\lambda \delta_{m=0} + \omega_{\text{aniso}}^\lambda \left\{ D^2_{0,-m}(\Omega^\lambda_{\text{PR}}) - \frac{\eta^\lambda}{\sqrt{6}}[D^2_{-2,-m}(\Omega^\lambda_{\text{PR}}) + D^2_{2,-m}(\Omega^\lambda_{\text{PR}})] \right\} d^2_{-m,0}(\beta_{\text{RL}}) \quad (3)$$

For the chemical shielding interaction ($\lambda = A$ or B), the isotropic and anisotropic frequency components are given by $\omega^\lambda_{\text{iso}} = -\omega_0\sigma^\lambda_{\text{iso}}$ and $\omega^\lambda_{\text{aniso}} = -\omega_0\sigma^\lambda_{\text{aniso}}$, respectively, with the isotropic chemical shift, the chemical shielding anisotropy, and the asymmetry parameter related to the principal elements of the shielding tensor according to $\sigma^\lambda_{\text{iso}} = (\sigma^\lambda_{xx} + \sigma^\lambda_{yy} + \sigma^\lambda_{zz})/3$, $\sigma^\lambda_{\text{aniso}} = \sigma^\lambda_{zz} - \sigma^\lambda_{\text{iso}}$, and $\eta^\lambda = (\sigma^\lambda_{yy} - \sigma^\lambda_{xx})/\sigma^\lambda_{\text{aniso}}$ ($|\sigma^\lambda_{zz} - \sigma^\lambda_{\text{iso}}| \geq |\sigma^\lambda_{xx} - \sigma^\lambda_{\text{iso}}| \geq |\sigma^\lambda_{yy} - \sigma^\lambda_{\text{iso}}|$). Likewise, for the coupling interactions we have $\omega^J_{\text{iso}} = \pi J_{AB}$, $\omega^J_{\text{aniso}} = 0$, $\omega^D_{\text{iso}} = 0$, $\omega^D_{\text{aniso}} = b_{AB} = -\mu_0\gamma_A\gamma_B\hbar/(4\pi r^3_{AB})$, and $\eta^D = 0$, where J_{AB}, b_{AB}, and r_{AB} refer to the scalar indirect coupling, the dipolar coupling, and the internuclear distance, respectively. $d^2_{-m,0}$ is a reduced Wigner element and $D^2_{p,q}(\Omega^\lambda_{\text{PR}})$ is an element of the second-rank Wigner matrix describing transformation from the principal axis frame P^λ of the interaction λ through a crystal-fixed frame C to the rotor-fixed frame R:

$$D^2_{p,q}(\Omega^\lambda_{\text{PR}}) = \sum_{k=-2}^{2} D^2_{p,k}(\Omega^\lambda_{\text{PC}}) D^2_{k,q}(\Omega^\lambda_{\text{CR}}) \quad (4)$$

To facilitate direct relation of the Euler angles for the chemical shielding tensors to the molecular frame, the crystal-fixed frame is arbitrarily defined coincident with the principal axis frame of the dipolar interaction, i.e., $\Omega^D_{\text{PC}} = (0,0,0)$. In this case, the relative orientation of the anisotropic chemical shielding and dipolar coupling tensors is described by five Euler angles α^A_{PC}, β^A_{PC}, α^B_{PC}, β^B_{PC}, and $\gamma^A_{\text{PC}} - \gamma^B_{\text{PC}}$ defined in Figure 1a. This takes into account that rotations of all tensors about the internuclear axis cannot be distinguished by regular ^{31}P MAS NMR.

Based on the Hamiltonian in eq 1, the powder spectrum of the spin pair is straightforwardly obtained as the Fourier transform of

$$s(t) = \sum_{\Omega_{\text{CR}}} \text{Tr}\{(S_A^+ + S_B^+)U(t,0)(S_{Ax} + S_{Bx})U^\dagger(t,0)\} \quad (5)$$

where the summation indicates averaging over all uniformly distributed crystallite orientations and the propagator is related to the Hamiltonian according to

$$U(t,0) = \hat{T}\exp\{-i\int_0^t H(t')\mathrm{d}t'\} \quad (6)$$

with $\hat{T}$ being the Dyson time-ordering superoperator.

To extract accurate values for all or some of the 13 parameters describing magnitudes and relative orientations of the chemical shielding and coupling tensors, a simulation program based on eq 5 was combined with the MINUIT optimization package.[18] This combination allowed efficient least-squares iterative fitting to experimental ^{31}P MAS spectra using various combinations of Monte Carlo, simplex, and steepest-descend optimization procedures which proves convenient for iterative fitting involving large numbers of variables. In practice, it is often possible to significantly reduce the number of free variables either because specific values may be known a priori from other sources (often magnitudes of tensorial interactions) or because known symmetries of the local structure impose restrictions on the relative orientation of the anisotropic interaction tensors. In the present study, addressing $n = 0$ rotational resonance effects within isolated ^{31}P$-^{31}$P spin pairs, it is relevant to discuss three cases of symmetry operations which may be used as an ingredient in, or confirmed by, iterative fitting of ^{31}P MAS spectra.

(18) James, F.; Roos, M. *MINUIT computer code*; Program D-506, CERN, Geneva: 1977; *Comput. Phys. Comm.* **1975**, *10*, 343.

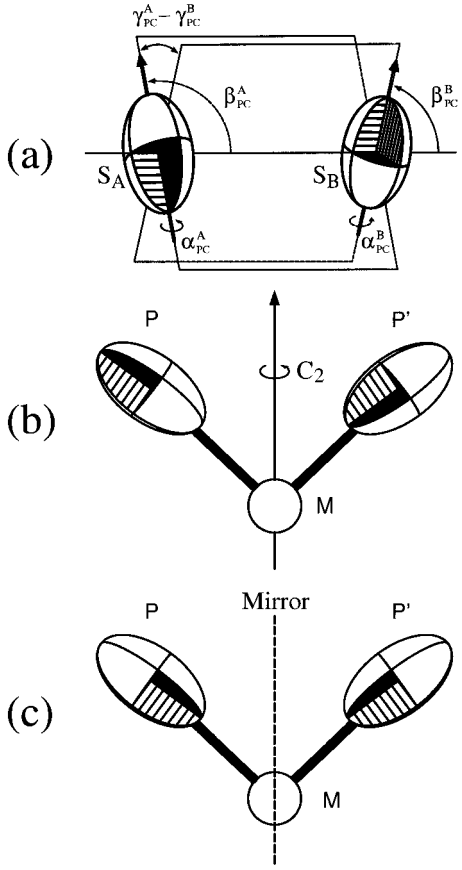

Figure 1. (a) Definition of Euler angles describing the relative orientation of chemical shielding tensors for S_A-S_B spin pairs relative to the principal axis frame of the dipolar interaction ($\Omega^D_{\text{PC}} = (0,0,0)$). (b and c) Representative tensor orientations corresponding to (b) C_2 symmetry with respect to the axis bisecting the P−M−P bond angle, and (c) reflection symmetry imposed by a mirror plane perpendicular to the P−P axis.

For ^{31}P$-^{31}$P spin pairs displaying identical isotropic chemical shifts in molecular solids such as **1**−**3**, one may encounter inversion symmetry, C_2 symmetry, or reflection symmetry relating the two anisotropic chemical shielding tensors. In the presence of inversion symmetry, the two ^{31}P chemical shielding tensors not only display identical magnitudes but also identical orientations. Under these circumstances the Hamiltonian behaves inhomogeneously,[4] implying that the spinning sidebands observed in the ^{31}P MAS NMR spectra will be structureless. This unique behavior is readily identified by MAS NMR and shall not be further elaborated on. For those cases where C_2 symmetry around an axis bisecting the P−M−P (M = metal) bond angle exists, the orientation of the two ^{31}P chemical shielding tensors is related according to

$$\alpha^B_{\text{PC}} = \alpha^A_{\text{PC}}, \quad \beta^B_{\text{PC}} = \beta^A_{\text{PC}} + \pi, \quad \gamma^B_{\text{PC}} = \gamma^A_{\text{PC}} + \pi \quad (7)$$

as illustrated for a typical P−M−P (M = metal) coordination fragment in Figure 1b. If the two shielding tensors are related

by reflection symmetry involving a mirror plane perpendicular to the internuclear axis, the corresponding relations for *A* and *B* are (see Figure 1c)

$$\alpha_{PC}^{B} = -\alpha_{PC}^{A}, \quad \beta_{PC}^{B} = \pi - \beta_{PC}^{A}, \quad \gamma_{PC}^{B} = \gamma_{PC}^{A} \qquad (8)$$

For a two-spin system of two crystallographically equivalent sites, there exists a principal degeneracy: β and $\pi - \beta$ are related by symmetry (or, in other words: the labels *A* and *B* are interchangeable). Hence, there will always be two indistinguishable solutions, and the choice of β over $\pi - \beta$, or vice versa, is completely arbitrary in the absence of further anisotropic interactions (or further independent constraints in general). For the two cases described by eqs 7 and 8, the number of variables describing the relative orientation of the chemical shielding tensors with respect to the $^{31}P-^{31}P$ dipolar axis reduces to two.

Results and Discussion

The $^{31}P-^{31}P$ spin pairs in compounds **1**−**3** have in common that they represent $n = 0$ rotational resonance cases in a selection of typical transition-metal phosphine complexes containing a P_2M moiety. The three cases differ from each other with respect to the metal M (M = Hg (**1**), Ni (**2**), Pd (**3**)) and the P−M−P bond lengths and angles present. Correspondingly, the $^{31}P-^{31}P$ spin pairs in **1**−**3** cover a range of relative magnitudes and orientations of chemical shielding, *J* coupling, and dipolar coupling interactions. The single-crystal X-ray structures of **1**[19] and **2**[14] have been determined. **1**,[3,10,12] **2**,[14] and **3**[11] have previously been examined by ^{31}P solid-state NMR.

Compound 1, $Hg(NO_3)_2(PPh_3)_2$. For **1** a single-crystal ^{31}P NMR study has been reported.[3] **1** has been chosen as an example also in our study, so that accuracy and efficiency of the two different approaches may be compared. At high MAS frequencies, we find one isotropic ^{31}P resonance for solid **1**, with $\sigma_{iso} = -40.1$ ppm in very good agreement with data reported in the literature.[10] The known single-crystal structure of **1**,[19] in conjunction with the magnitude of $J = 250$ Hz previously determined from *J* recoupling patterns in ^{31}P MAS spectra of **1**[10] provide the initial set of parameters for the simulation of ^{31}P MAS spectra of **1**. The two crystallographically equivalent P sites in the molecule are related by a C_2 symmetry axis bisecting the P−Hg−P angle (131.76°), the internuclear P−P distance in **1** is 447 pm,[19] and the dipolar coupling constant calculated from this distance is $b_{AB}/2\pi = -220$ Hz.

An experimental ^{31}P MAS NMR spectrum of **1** is displayed in Figure 2a ($\omega_0/2\pi = -121.5$ MHz, $\omega_r/2\pi = 4167$ Hz). Using C_2 symmetry and the known values of σ_{iso}, *J*, and b_{AB} as initial parameters, the simulated spectrum shown in Figure 2c, described by the parameters given in Table 1, is obtained as the best fit for the ^{31}P MAS NMR spectrum of **1**.

Note that all spectral features in the experimental ^{31}P MAS spectrum, originating from heteronuclear coupling to ^{199}Hg and ^{201}Hg in isotopomers containing $(^{31}P)_2{}^{199}Hg$ or $(^{31}P)_2{}^{201}Hg$ three-spin systems (marked * and + in Figure 2b, respectively) are well separated from all spectral contributions originating from those (majority) isotopomers in **1** which only contain isolated ^{31}P spin pairs. By appropriately adjusting the MAS frequencies used, it is for **1** (and, more generally, for similar transition-metal phosphine complexes containing magnetically active metal nuclei of low natural abundance) usually straightforward to avoid overlap. The theoretical spectrum shown in (c) corresponds to the best fit parameters (Table 1) for the isotopomers of **1** containing isolated ^{31}P spin pairs only. The orientation of the ^{31}P chemical shielding tensors within the molecular frame of **1**, according to Table 1, is illustrated in the ORTEP-like plot in Figure 3a.

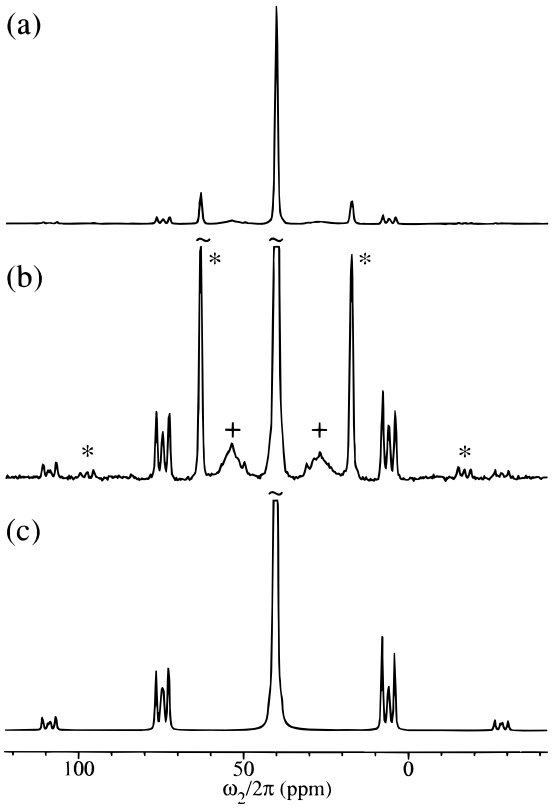

Figure 2. Experimental and theoretical ^{31}P MAS NMR spectra of $Hg(PPh_3)_2(NO_3)_2$, **1**. (a) Experimental spectrum recorded using $\omega_0/2\pi = -121.5$ MHz (7.0 T) and $\omega_r/2\pi = 4167$ Hz. (b) Same experimental spectrum, with the vertical axis expanded to allow for easier comparison of spinning sideband patterns of experimental and theoretical spectrum, displayed in (c). The theoretical spectrum shown in (c) corresponds to the optimum parameters given in Table 1. Note that all spectral features in the experimental ^{31}P MAS spectrum, originating from heteronuclear coupling to ^{199}Hg and ^{201}Hg in isotopomers containing $(^{31}P)_2{}^{199}Hg$ (marked by * in (b)), or $(^{31}P)_2{}^{201}Hg$ (marked by + in (b)) three-spin systems, are not reproduced in the theoretical spectrum shown in (c).

To further examine the dependence of the theoretical spectra on the orientational parameters of the chemical shielding tensors, the chi-square (χ^2) deviation between experimental and theoretical spectra was calculated for the values given in Table 1, with the angles α_{PC}^{A} and β_{PC}^{A} varied from 0° to 180° (see Figure 4).

While χ^2 reveals two relatively sharp minima at $\alpha_{PC}^{A} = 45°$ and 135° (Figure 4a), Figure 4b shows two minima ($\beta_{PC}^{A} = 38°$ and 52°) in a broad "minimum region" for β_{PC}^{A}, ranging from about 35° to 55° (or, alternatively from 125° to 145°). The minimum for $\beta_{PC}^{A} = 38°$ corresponds to an orientation of the most shielded tensor component nearest to the Hg−P bond direction, with a deviation of 14° from this molecular direction. The second minimum for $\beta_{PC}^{A} = 52°$ would place the least shielded tensor component nearer to the Hg−P bond direction than would be the most shielded tensor component. From iterative fitting of ^{31}P MAS NMR spectra of **1**, the two orientations corresponding to the two minima for β_{PC}^{A} cannot be significantly distinguished. However, the result from iterative fitting of ^{31}P MAS NMR spectra of **1** is in agreement with the results of a previously reported single crystal NMR study of **1**.[3] The minimum for $\beta_{PC}^{A} = 38°$ is precisely the orientation

(19) Buergi, H. B.; Fischer, E.; Kunz, R. W.; Parvez, M.; Pregosin, P. S. *Inorg. Chem.* **1982**, *21*, 1246.

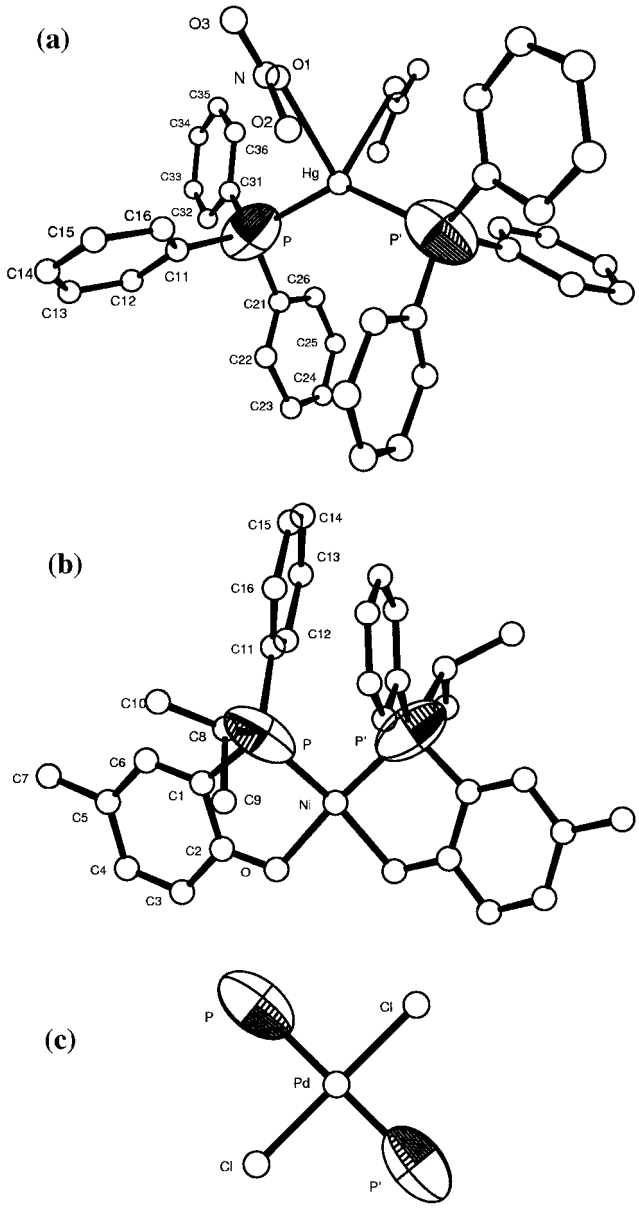

Figure 3. ORTEP-like plots illustrating the orientation of the ^{31}P chemical shielding tensors within the molecular frame of **1** (a), **2** (b), and **3** (c) as determined by ^{31}P MAS NMR (see Table 1). The drawing for **3** (c) utilizes an idealized square-planar coordination, the atomic coordinates in (a) and (b) have been taken from the X-ray diffraction studies of Buergi et al.[19] (a) and Heinicke et al.[14](b).

also given in the single-crystal NMR study. Within the error limits given for the single-crystal ^{31}P NMR data, even if we would take the entire ^{31}P MAS fitting "minimum region" as $\beta^A_{PC} = 45 \pm 10°$ (corresponding to an angle of $21 \pm 10°$ between the most shielded component of the ^{31}P chemical shielding tensor and the Hg−P bond direction in **1**), there would still be agreement between single-crystal NMR results and the results of iterative fitting of ^{31}P MAS NMR spectra of **1** with respect to the orientation of the most shielded tensor component.

Having demonstrated that iterative fitting of ^{31}P MAS NMR spectra yields results which are comparable to the information obtained from single-crystal NMR, we will next consider a case for which the single-crystal X-ray structure is known but for which no single-crystal ^{31}P NMR data exist.

Compound 2, $NiP_2C_{32}H_{36}O_2$. **2** crystallizes in space group *C*2/*c*; the Ni atom resides in an only slightly distorted square-planar P_2NiO_2 coordination sphere. The two crystallographically equivalent P atoms in the molecule are related by C_2 symmetry,

Table 1. Parameters for Dipolar Coupling, *J* Coupling, and Chemical Shielding Tensors for the Isolated $^{31}P-^{31}P$ Spin Pairs in Compounds **1**−**3** Determined by Iterative Fitting of ^{31}P MAS NMR Spectra[a]

	1	**2**	**3**
$b_{AB}/2\pi$ (Hz)	-220 ± 20	-584 ± 20	-200 ± 50
J_{AB} (Hz)	$+280 \pm 20$	-74 ± 5	$+537 \pm 10$
ω^A_{iso} (ppm)	-40.1	-47.1	-10.9
ω^A_{aniso} (ppm)	39 ± 7	65 ± 2	-47 ± 2
η^A	0.67 ± 0.1	0.56 ± 0.1	0.35 ± 0.1
$\alpha^{A\ b}_{PC}$	45 ± 10	21 ± 10	63 ± 10
$\beta^{A\ b,c}_{PC}$	38 ± 3^d	35 ± 3	84 ± 2

[a] Euler angles (deg) for the two shielding tensors *A* and *B* are mutually related by C_2 symmetry for all three compounds **1**−**3** (see eq 7, γ^A_{PC} arbitrarily set to 0) and to the principal axis frame of the dipolar interaction, i.e., $\Omega^D_{PC} = (0,0,0)$. [b] See also Figures 4, 6, and 9. [c] Only one of the two principally possible choices, β and $\pi - \beta$, is listed in the table. [d] Second minimum for $\beta^A_{PC} = 52 \pm 3°$ (see text).

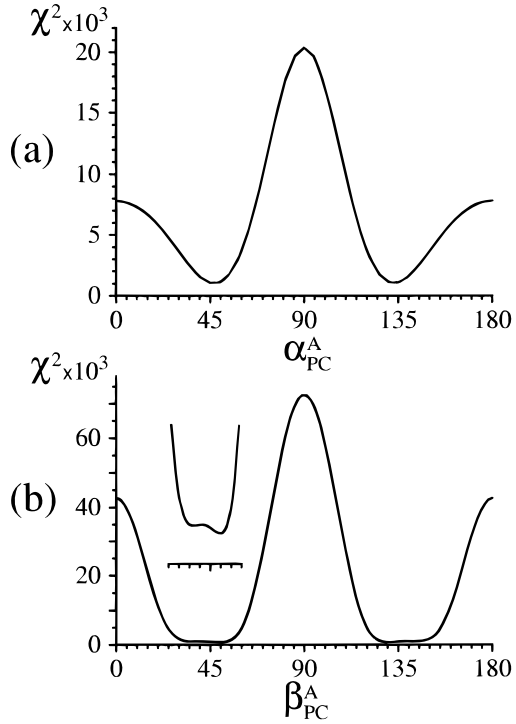

Figure 4. Chi-square (χ^2) deviation between experimental and simulated ^{31}P MAS NMR spectra plotted as a function of angles (a) α^A_{PC} and (b) β^A_{PC} [deg] for compound **1**. The plots use the definition $\chi^2 = kR$, where $R = \sum_{j=1}^{N} |I_j^{exp} - I_j^{sim}|^2$ is the least-squares difference between intensities of experimental (I_j^{exp}) and calculated (I_j^{sim}) spectra. $k = (N-N_{par})/R_{min}$, where R_{min} is the least-squares difference for the optimum fit, *N* the number of spectral points, and N_{par} the number of variables. The plots are based on the parameters given in Table 1, except for the respective variable parameter.

with the axis of symmetry bisecting the P−Ni−P bond angle (97.9°). The P−P internuclear distance in **2** as determined by single-crystal X-ray diffraction is 323 pm. ^{31}P MAS spectra of **2** obtained at high MAS frequencies display one isotropic ^{31}P resonance ($\sigma_{iso} = -47.1$ ppm) while—in accord with the single-crystal X-ray diffraction results—at lower MAS frequencies complex lineshapes are observed in the ^{31}P MAS spectra of **2**.[14] Hence, the starting point for simulation of ^{31}P MAS spectra of **2** is the known symmetry operation relating the two ^{31}P chemical shielding tensors and a dipolar coupling constant $b_{AB}/2\pi = -584$ Hz.

Experimental ^{31}P MAS NMR spectra of **2** ($\omega_0/2\pi = -202.5$ MHz and $\omega_r/2\pi = 2500$ Hz; and $\omega_0/2\pi = -40.5$ MHz and

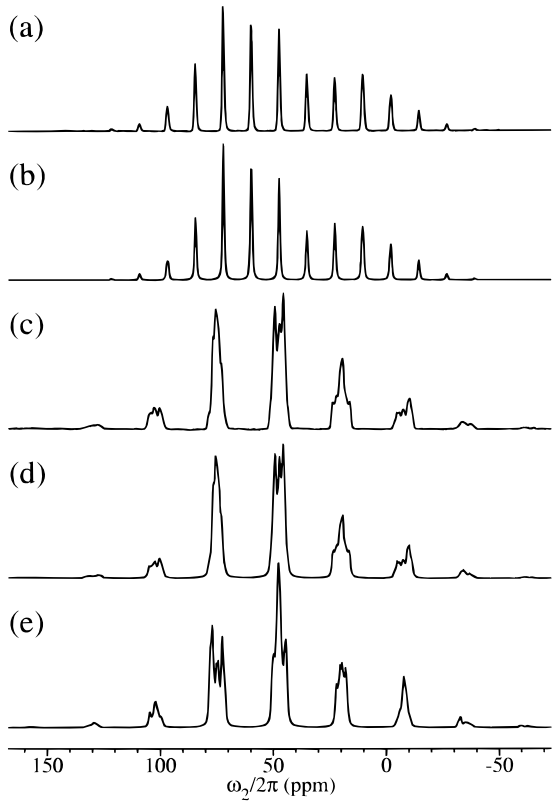

Figure 5. Experimental and theoretical ^{31}P MAS NMR spectra of $NiP_2C_{32}H_{36}O_2$, **2**. (a and c) Experimental spectra obtained at (a) $\omega_0/2\pi = -202.5$ MHz (11.7 T) and $\omega_r/2\pi = 2500$ Hz and (b) $\omega_0/2\pi = -40.5$ MHz (2.35 T) and $\omega_r/2\pi = 1111$ Hz. (b and d) Theoretical spectra corresponding to (a) and (c), respectively, and representing the optimum parameters as given in Table 1. (e) Theoretical spectrum using identical parameters as (d) but reversed sign of J_{AB}.

$\omega_r/2\pi = 1111$ Hz) are depicted in Figure 5 (parts a and c, respectively). Comparing these two ^{31}P MAS NMR spectra demonstrates how strongly the spectral lineshape is influenced by the combined effects of external experimental parameters $\omega_0/2\pi$ and $\omega_r/2\pi$. The location of the most informative (or, likewise, of a potentially misleading) $\omega_0/2\pi$ and $\omega_r/2\pi$ window with respect to the extraction of the anisotropic interaction parameters of a given spin pair, in turn, depends on the relative magnitudes and orientations of these interactions. For compound **2**, ^{31}P MAS NMR spectra obtained at $\omega_0/2\pi = -202.5$ MHz are suitable to obtain an *estimate* of the magnitude of the chemical shielding tensor principal values, the spectra obtained at high magnetic field strength are dominated by chemical shielding anisotropy and can thus provide initial input parameters for iterative fitting of ^{31}P MAS NMR spectra obtained at lower external magnetic field strength. For **2**, spectra obtained at much lower external magnetic field strength (see Figure 5c) are more suitable for the extraction of orientational parameters by means of iterative fitting, owing to the complex shapes of all spinning sidebands occurring under these conditions. In fact, selective scaling of the various interactions by the appropriate choice of external magnetic field strengths and MAS frequencies can be used advantageously to achieve better accuracy of the data extracted from iterative spectral lineshape fitting procedures. Calculated spectra, corresponding to the ^{31}P spin-pair parameters of solid **2** obtained as the best fit, are shown in Figure 5 (parts b and d, respectively,) in comparison to the respective experimental ^{31}P MAS NMR spectra. The best fit ^{31}P NMR data for **2** are listed in Table 1, the resulting orientation of the two ^{31}P chemical shielding tensors in the molecular frame of **2** are illustrated in the ORTEP-like plot in Figure 3b. Magnitude and

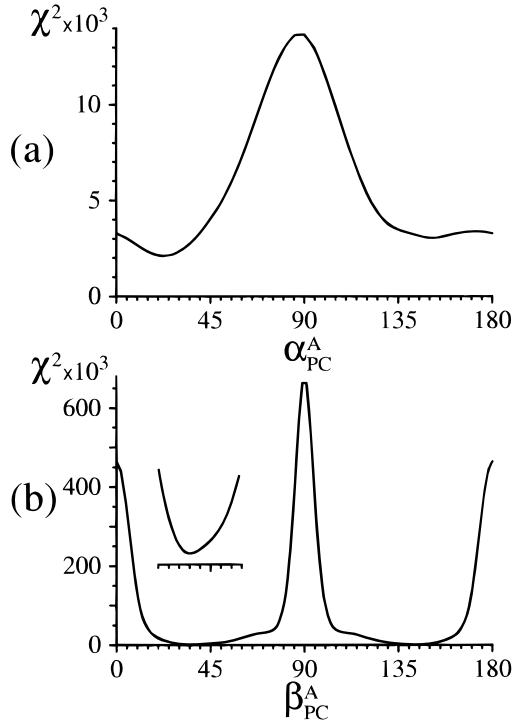

Figure 6. Chi-square (χ^2) deviation between experimental (cf. Figure 5c) and simulated (cf. Figure 5d) 2.35 T ^{31}P MAS NMR spectra for compound **2**, plotted as a function of (a) α^A_{PC} and (b) β^A_{PC}; definitions as given in Figure 4.

sign of J_{AB} in **2** are obtained from iterative fitting (see Table 1, $J_{AB} = -74$ Hz); despite J being the interaction of smallest magnitude, the spectral lineshape of ^{31}P MAS NMR spectra of **2** is highly sensitive toward the sign of J. This is illustrated in Figure 5e where a spectrum is shown, calculated with the best fit parameters in Table 1 where solely the sign of J has been changed to positive. Simulations of ^{31}P MAS NMR spectra of **2** where $b_{AB}/2\pi$ is not fixed to the value calculated from the single-crystal X-ray structure but is a free fit parameter essentially yield the same parameters as do simulations with $b_{AB}/2\pi$ fixed to the value calculated from the known internuclear P−P distance in **2**. From this we may conclude that (i) also in the absence of knowledge of the single-crystal X-ray structure of **2** we would have obtained an accurate measure of the P−P distance from iterative fitting of ^{31}P MAS NMR spectra of **2** and (ii) this finding further supports the tacitly made assumption that anisotropy of J_{AB} is indeed negligible for **2**.

For the best fit of experimental ^{31}P MAS NMR spectra of **2** we find orientational parameters $\alpha^A_{PC} = 21°$ and $\beta^A_{PC} = 35°$ (see Table 1), where the solution $\beta^A_{PC} = 35°$ corresponds to an orientation of the most shielded tensor component very near (deviation of 6°) to the Ni−P bond direction. This orientation of the ^{31}P chemical shielding tensors in the molecular frame of **2** is illustrated in Figure 3b. Closer inspection of further bond lengths and bond angles in the immediate neighborhood of the P atoms in the single-crystal structure of **2**[14] gives no clue to any specific, immediately obvious preferred direction with respect to the remaining two shielding tensor components; no symmetry arguments may be used to even qualitatively comment on the value found for $\alpha^A_{PC} = 21°$. In Figure 6 are shown chi-square (χ^2) plots of the deviation between experimental and simulated spectra, for α^A_{PC} and for β^A_{PC}. The χ^2 range for α^A_{PC} is found to be fairly shallow; χ^2 plotted as a function of β^A_{PC} shows a seemingly very broad minimum region, though with a distinct and much narrower, proper minimum near 35° (and, of course, an indistinguishable minimum for 145°). Because of

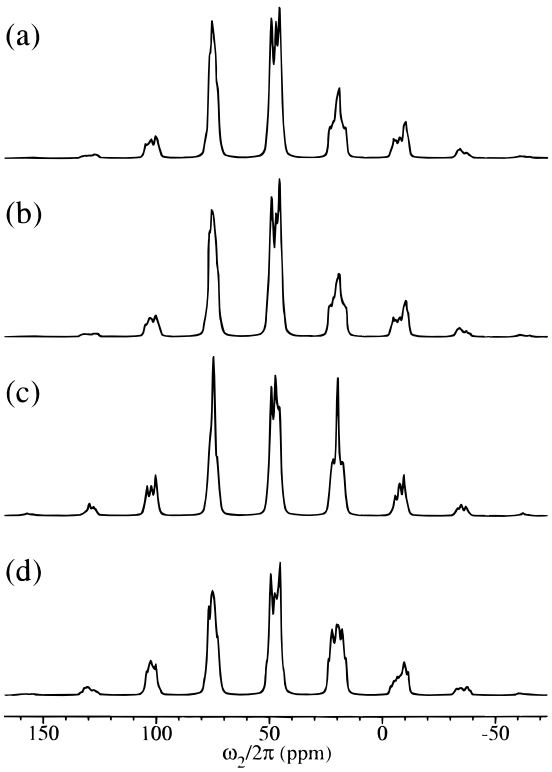

Figure 7. Simulated 2.35 T ^{31}P MAS spectra based on the optimum fit parameters for **2** given in Table 1. Simulation assuming (a) C_2 symmetry and (b) a mirror plane as the applicable symmetry operation (cf. Figure 1 (parts b and c)). (c and d) Simulations where $\alpha^A_{PC} = 45°$, and $\eta^A = \eta^B = 1$ have been misadjusted deliberately for the two different symmetry operations connecting the two chemical shielding tensors: (c) C_2 symmetry and (d) mirror plane.

the considerable amount of fine structure of all spinning sidebands in experimental ^{31}P MAS spectra of **2** obtained at low external magnetic field strengths, even small deviations from this narrow minimum region can be significantly detected in simulated spectra. The precise location of the optimum value for α^A_{PC} is less well-defined.

For iterative lineshape fitting of ^{31}P MAS NMR spectra of **2**, no assumptions concerning the symmetry operation relating the two ^{31}P chemical shielding tensors had to be made because of the known single-crystal structure of this compound. With a view to future applications of iterative lineshape fitting of ^{31}P MAS NMR spectra for cases of unknown single-crystal X-ray structure, it seems worthwhile to explore the possibilities to distinguish between C_2 symmetry axis or a mirror plane (see Figure 1) as the applicable symmetry operation relating the two ^{31}P chemical shielding tensors. In Figure 7 simulated spectra, based on the parameters for **2**, for these two cases of symmetry operations are depicted.

The spectrum calculated for C_2 symmetry (see Figure 7a) corresponds to the best fit parameters for **2**, while the spectrum calculated assuming a mirror plane as the appropriate symmetry operation (see Figure 7b) was obtained using identical parameters and merely adjusting the relationships between $\alpha^A_{PC}/\alpha^B_{PC}$ and $\beta^A_{PC}/\beta^A_{PC}$ according to eq 8. No attempt has been made to obtain a "best fit" of the experimental ^{31}P MAS NMR spectra of **2** for this "wrong" symmetry operation. No significant differences in lineshapes are found between these two cases. That this is not necessarily and not always the case is illustrated in Figure 7c,d. The two simulated spectra shown there use deliberately misadjusted simulation parameters ($\eta^A = \eta^B = 1$ and $\alpha^A_{PC} = 45°$) for both cases, and there are distinct differences in the spectral lineshapes for the two different symmetry operations. Realistically, we have to conclude from the examples given in Figure 7 that iterative lineshape fitting in fortunate cases may allow distinction of applicable local symmetry operations, while claiming that this should be generally possible would seem an exaggeration.

Compound 3, $Pd(P^nBu_3)_2Cl_2$. Other than for **1** and **2**, the single-crystal X-ray structure of **3** is unknown. At high MAS frequencies one ^{31}P resonance is observed in ^{31}P MAS spectra of **3** ($\sigma_{iso} = -10.9$ ppm), pointing to crystallographic equivalence of the two P atoms in the molecule. A square-planar *trans*-P_2PdCl_2 arrangement with a pair of crystallographically equivalent P atoms would not a priori exclude inversion symmetry as the appropriate symmetry operation relating these two P sites. The occurrence of *J* recoupling in ^{31}P MAS spectra of **3** obtained at lower MAS frequencies, however, does exclude inversion symmetry,[11] while the occurrence of *J* recoupling per se does not exclude a square-planar *cis*-P_2PdCl_2 arrangement. Ascribing a square-planar *trans*-P_2PdCl_2 configuration to this compound is, however, a reasonable assumption: a magnitude of $J = 537$ Hz has been determined from *J* recoupling patterns for **3**;[11] this magnitude of *J* is typical for *trans*-P_2Pd arrangements in many Pd(II) phosphine complexes.[20] Taking the *trans*-P_2Pd arrangement as sufficiently well established for **3**, in the absence of single-crystal X-ray diffraction information we are left with two a priori possible symmetry operations relating the two P sites in the molecule: either a C_2 symmetry axis, coincident with the Cl−P−Cl bond direction, or a mirror plane perpendicular to the P−Pd−P bond direction and containing the Cl−Pd−Cl bond axis. Since such a mirror plane would require an energetically highly unfavorable eclipsed conformation of the six bulky ^{n}Bu ligands in the molecule (while C_2 symmetry does allow for an energetically much more favorable staggered conformation), it seems reasonable to assume C_2 as the symmetry operation relating the two P sites in the molecule. We may estimate the P−P internuclear distance in **3** as ca. 450 pm, corresponding to a dipolar coupling constant $b_{AB}/2\pi \approx -230$ Hz. Assumed C_2 symmetry, an estimated internuclear P−P distance, and the previously determined magnitude of *J* represent the starting conditions for the simulation of ^{31}P MAS spectra of **3**.

Figure 8a shows an experimental ^{31}P MAS NMR spectrum of **3** ($\omega_0/2_\pi = -202.5$ MHz), obtained at a spinning frequency of $\omega_r/2\pi = 2002$ Hz, which represents a spinning frequency regime where *J* recoupling is clearly observable. The spectrum shown in Figure 8b was determined as best fit, with the parameters given in Table 1 and a C_2 symmetry axis, bisecting the P−Pd−P bond angle. The chi-square (χ^2) deviation between experimental and theoretical spectra as a function of the angles α^A_{PC} and β^A_{PC} is shown in Figure 9. Apart from the respective angles, the plots employ the values given in Table 1. Figure 9a shows a minimum of χ^2 for the angle $\alpha^A_{PC} = 63°$, while Figure 9b reveals two clearly defined minima for $\beta^A_{PC} = 2°$ (178°) and 84° (96°). These angles β of 2° and 84°, however, describe two quite different chemical shielding tensor orientations. While a value of $\beta^A_{PC} = 2°$ would imply that the least shielded component of the chemical shielding tensor lies along the P−Pd bond direction, a value of 84° would correspond to the most shielded tensor component near to the P−Pd bond direction. The two minima are of similar χ^2 quality. In order to resolve this remaining ambiguity from iterative lineshape fitting of ^{31}P MAS NMR spectra of **3**, a static 2D ^{31}P spin-

(20) Pregosin, P. S.; Kunz, R. W. ^{31}P and ^{13}C NMR of Transition Metal Complexes. In *NMR Basic Principles Progress*; Springer: Berlin, 1979; Vol. 16.

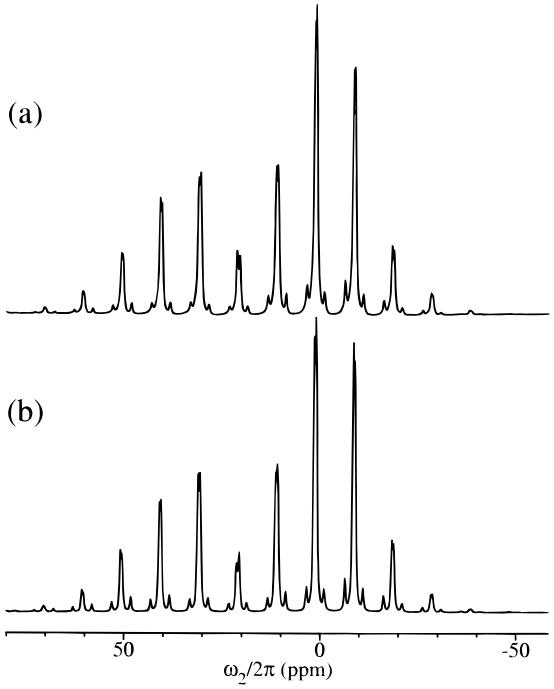

Figure 8. Experimental and theoretical ^{31}P MAS NMR spectra of *trans*-Pd(P^{n}Bu$_3$)$_2$Cl$_2$, **3**. (a) Experimental spectrum ($\omega_0/2\pi = -202.5$ MHz (11.7 T) and $\omega_r/2\pi = 2002$ Hz). (b) Theoretical spectrum using the parameters given in Table 1 and a C_2 symmetry axis, bisecting the P−Pd−P bond angle.

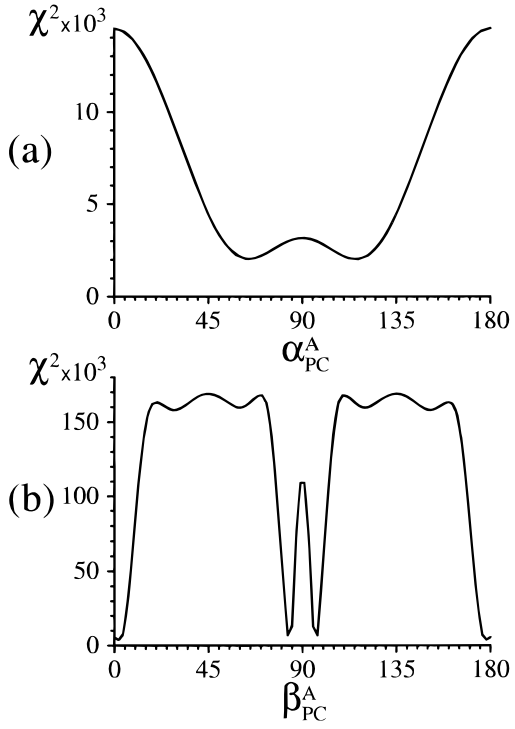

Figure 9. Chi-square (χ^2) deviation between experimental and calculated ^{31}P MAS NMR spectra vs (a) α^A_{PC}, and (b) β^A_{PC} for compound **3**. Apart from the respective variable parameter, the plots employ the parameters given for **3** in Table 1; the definitions are as in Figure 4.

echo experiment[2] was obtained and simulated. The contour plot of the experimental spectrum ($\omega_0/2\pi = -81.0$ MHz) is shown in Figure 10a. Simulations of the spin-echo experiment on **3** were performed using the parameters obtained from iterative fitting of the ^{31}P MAS NMR spectra of **3** (see Table 1), except for β^A_{PC}, which was varied from 0° to 180°. The resulting

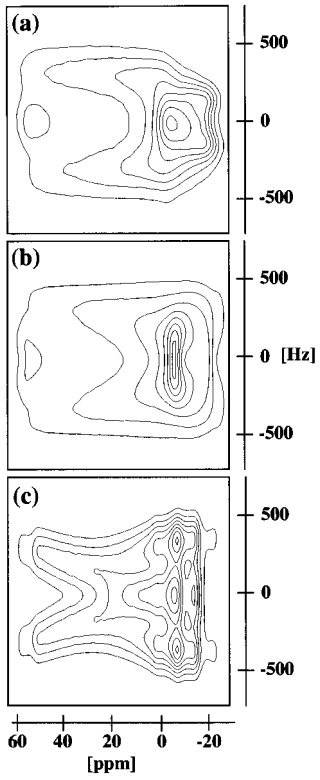

Figure 10. Experimental and theoretical 2D ^{31}P spin-echo NMR spectra of a static powder of **3**. (a) Experimental spectrum ($\omega_0/2\pi = -81.0$ MHz (4.7 T)). (b and c) Theoretical spectra calculated using C_2 symmetry and the parameters given in Table 1. (b) Contour plot of calculated spectrum for $\beta^A_{PC} = 85°$ and (c) contour plot of calculated spectrum for $\beta^A_{PC} = 2°$.

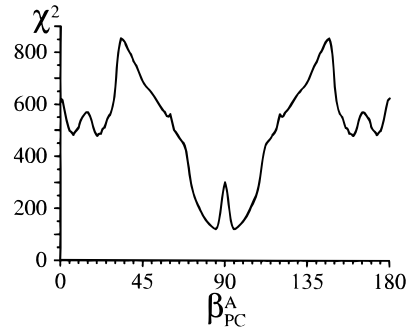

Figure 11. Chi-square (χ^2) deviation between experimental and calculated 2D ^{31}P spin-echo spectra vs β^A_{PC} for compound **3**. The plot uses the parameters from Table 1, except for the variable parameter, and the vertical scale is in arbitrary units.

chi-square plot is shown in Figure 11. The curve reveals only one minimum at $\beta^A_{PC} = 85°$ (95°). A value of $\beta^A_{PC} = 2°$ is clearly excluded by the simulation of the 2D spin-echo experiment, as can also be seen by inspection of the contour plots of the simulated spin-echo spectra of **3** for β^A_{PC} values of 85° and 2° in Figure 10 (parts b and c, respectively). Combined consideration of simulations of the 2D spin-echo experiment and of the results of iterative fitting of ^{31}P MAS NMR spectra clearly selects the value $\beta^A_{PC} = 84°$ (96°) as the correct solution, meaning that the most shielded component of the two chemical shielding tensors is oriented next to the P−Pd bond direction within ±5°. If an idealized local symmetry of a R$_3$P−M unit only would have been considered, in conjunction with qualitative inspection of the nearly axially symmetric ^{31}P chemical shielding tensor for **3**, where the "nearly unique" chemical shielding tensor component is the least shielded

component, a completely wrong conclusion about the orientation of the two ^{31}P chemical shielding tensors in the molecular frame of **3** would have been drawn. A schematic illustration of the orientation of the ^{31}P chemical shielding tensors in an (idealized) molecular *trans*-P_2PdCl_2 frame of **3** is given in Figure 3c.

The single-crystal X-ray structure of **3** is not known, hence information about the intermolecular P−P distance has to be derived from the results of iterative fitting of the ^{31}P MAS NMR spectra. A value of $b_{AB}/2\pi = -200$ Hz from the best fit (see Table 1) corresponds to a P−P distance of 462 pm, in fair agreement with bond distances known from X-ray diffraction investigations of other, related Pd(II)−phosphine complexes.[15b] This calculation of the P−P distance in **3** suffers from an uncertainty: it neglects possible contributions from anisotropy of J_{AB}, and we have little to no means to soundly evaluate this degree of uncertainty. While, within experimental error, a significant contribution from anisotropy of J_{AB} could safely be excluded for compound **2**, the situation is slightly different for **3**, not only because of the unknown single-crystal X-ray structure for **3**: in this case J_{AB} no longer is the interaction with the smallest magnitude; in fact, the magnitude of J_{AB} amounts to nearly three times the magnitude of $b_{AB}/2\pi$.

Conclusions

It has been shown that iterative fitting of ^{31}P MAS NMR spectra of isolated ^{31}P spin pairs in typical transition-metal phosphine complexes provides an efficient and accurate method to determine magnitudes and relative orientations of the interaction tensors in these spin pairs. The accuracy achieved is comparable to the accuracy of single-crystal NMR studies of such spin systems. This aspect is important from a practical point of view, only rarely will such compounds of interest be available in the form of single crystals, suitable for solid-state NMR studies. In turn, often the single-crystal X-ray structure of such compounds will be known, and if polycrystalline powders are then sufficient to completely characterize the ^{31}P spin-pair parameters, a severe restriction with respect to availability of samples in a suitable form for solid-state NMR studies is lifted. For this particular class of chemicals, however, care needs to be exercised to ensure that the polycrystalline powders used for ^{31}P MAS NMR spectroscopy are identical in crystallographic space group with the material on which single-crystal X-ray diffraction investigations have been carried out, if single-crystal X-ray diffraction data are to be used as input parameters for NMR lineshape simulations: polymorphism is a common phenomenon for solid transition-metal phosphine complexes. Information from diffraction studies, that is knowledge of the internuclear distance within the spin pair, has an important role to play in the context of iterative fitting of ^{31}P MAS NMR spectra in yet another sense. As we have pointed out, possible contributions from anisotropy of J_{AB} cannot a priori be excluded and hence may introduce uncertainties in the determination of internuclear distances and relative tensor orientations from fitting of MAS NMR spectra. However, given a known internuclear distance, iterative fitting of MAS NMR spectra of, for instance, isolated ^{31}P spin pairs may represent a feasible route to more closely investigate aspects of anisotropy of J_{AB}.

^{31}P MAS or CP/MAS NMR spectra of the vast majority of transition−metal phosphine complexes are very easily obtained and, in most cases, only require modest amounts of experimental time to achieve an excellent signal-to-noise ratio. As we have pointed out, to determine highly accurate parameters from iterative lineshape fitting of ^{31}P MAS NMR spectra, it is necessary to have access to a fairly wide range of external magnetic field strengths. Given the speed and ease with which ^{31}P MAS NMR spectra of such compounds are obtained, this is not at all a severe restriction.

Finally, in this study we have only considered isolated ^{31}P spin pairs in fragments $(^{31}P)_2M$ where the two P sites in the molecule are crystallographically equivalent. The iterative lineshape fitting approach described here is, however, not restricted to this type of $n = 0$ rotational resonance spin-pair system. Also for the more general case of an isolated spin pair where the two chemical shielding tensors are no longer related by a symmetry operation, iterative lineshape fitting of ^{31}P MAS NMR spectra is a suitable method. Given the fairly large number of parameters characterizing this general kind of spin-pair system, it is desirable to have as many independently determined input parameters for spectral lineshape simulations as possible. Careful use of iterative fitting procedures is mandatory to avoid false minima, and iterative fitting, in turn, requires, e.g., efficient powder averaging methods in order to minimize the necessary amount of computation time.

Acknowledgment. Support of this work by Deutsche Forschungsgemeinschaft and Fonds der Chemischen Industrie is gratefully acknowledged. We would like to thank J. Heinicke, Greifswald, for the donation of compound **2** and H. Maisel, Bayreuth, for the preparation of compounds **1** and **3**. We thank Bruker Analytische Messtechnik, Karlsruhe, for providing generous access to the DSX 500 NMR spectrometer. N.C.N. acknowledges support from Carlsbergfondet.

JA970890R